

## Characterization of elastic properties in porous silicon carbide preforms fabricated using polymer waxes as pore formers

Siddhartha Roy, Karl Günter Schell, Ethel Claudia Bucharsky, Kay A. Weidenmann, Alexander Wanner, Michael J. Hoffmann

### Angaben zur Veröffentlichung / Publication details:

Roy, Siddhartha, Karl Günter Schell, Ethel Claudia Bucharsky, Kay A. Weidenmann, Alexander Wanner, and Michael J. Hoffmann. 2013. "Characterization of elastic properties in porous silicon carbide preforms fabricated using polymer waxes as pore formers." *Journal of the American Ceramic Society* 96 (7): 2269–75. <https://doi.org/10.1111/jace.12341>.

### Nutzungsbedingungen / Terms of use:

licgercopyright

Dieses Dokument wird unter folgenden Bedingungen zur Verfügung gestellt: / This document is made available under these conditions:

**Deutsches Urheberrecht**

Weitere Informationen finden Sie unter: / For more information see:

<https://www.uni-augsburg.de/de/organisation/bibliothek/publizieren-zitieren-archivieren/publiz/>



# Characterization of Elastic Properties in Porous Silicon Carbide Preforms Fabricated Using Polymer Waxes as Pore Formers

Siddhartha Roy,<sup>†</sup> Karl Günter Schell, Ethel Claudia Bucharsky, Kay André Weidenmann, Alexander Wanner, and Michael J. Hoffmann<sup>\*,\*\*</sup>

Institute for Applied Materials, Karlsruhe Institute of Technology, Karlsruhe 76131, Germany

**Thorough elastic analysis of porous silicon carbide preforms fabricated using two different polymer waxes as pore formers is carried out. Both the amount and the mixture ratio of the waxes were varied to fabricate preforms with different pore morphologies and porosities in the range of 27–67 vol%. Results show that both the longitudinal and the shear elastic constants decrease with increasing porosity. The rate of decrease in the elastic constants follows a model based on minimum solid area up to an intermediate porosity level. Uniaxial pressure applied prior to cold isostatic pressing and sintering significantly reduces the stiffness along the press direction. For the same initial powder mixture type, the elastic anisotropy of the preforms increases with an increase in the applied uniaxial pressure. The extent of anisotropy is strongly dependent on both the SiC/wax ratio as well as the mixture ratio between the two wax types. At low pore volume fractions a higher volume content of the smaller diameter wax and at high pore volume fractions a higher volume content of larger diameter wax lead to preforms with lowest anisotropy. A map is finally proposed to describe the dependence of the preform elastic properties on the type of initial powder mixture used.**

## I. Introduction

METAL/CERAMIC composites with an interpenetrating phase architecture (IPC) offer several advantages over particle reinforcement (PMC). These include higher stiffness and strength both at room and elevated temperatures,<sup>1</sup> lower coefficient of thermal expansion (CTE), thermal hysteretic behavior in terms of CTE,<sup>2,3</sup> etc. IPCs are typically fabricated by infiltrating a metallic alloy in an open porous ceramic preform.<sup>4,5</sup>

Because of their high thermal conductivity, low CTE, and lightweight, aluminum alloy matrix composites with silicon carbide (SiC) reinforcement are candidate materials for thermal management applications under weight critical conditions.<sup>6,7</sup> In a recent article,<sup>8</sup> the present authors reported a simple route for fabricating open porous SiC preforms with tailorable pore structure. Two different polymer wax types with very different particle diameters were used as pore formers. Both the total wax content and the mixture ratio of the two wax types were varied to alter both the pore volume fraction and the pore morphology in the final preforms. The mixture composed of SiC powder and the pore formers was first uniaxially pressed followed by cold isostatic pressing, heated to pyrolyse the polymer wax and finally sintered.

A first study of the elastic properties for preforms fabricated using only the 50/50 mixture of SiC/wax was carried out using ultrasound phase spectroscopy (UPS). Results showed that the ratio of the two wax types significantly influenced the pore morphology. Preforms fabricated using a mixture of the two wax types with a higher volume fraction of the larger wax particles were reported to have the best elastic properties along all directions.

Due to the large difference between the elastic properties of SiC reinforcement and the metallic phase in the composite, the preform anisotropy may significantly influence the elastic properties of the composite. The influence of preform characteristics on composite elastic properties has been discussed in detail in previous publications.<sup>9,10</sup> Therefore, understanding of the interrelationship between the preform microstructure and the elastic properties over a wide range of ceramic content is necessary before composites are fabricated. The aim of this work was to further understand the influence of the processing parameters on the elastic properties of the preforms. SiC preforms with a wide range of porosity (27–67 vol%) are fabricated. In-depth analysis of the influence of both the amount of porosity and the pore morphology on the preform elastic properties has been carried out. UPS has been used to measure the three longitudinal and the three shear elastic constants of the preforms. A map has been proposed to summarize the effect of the type of initial powder mixture on the preform elastic properties. In addition, to investigate the effect of the applied uniaxial pressure, elastic properties of preforms fabricated under different uniaxial pressures are determined.

## II. Experimental Procedure

### (1) Processing of Porous SiC

Detailed description of the processing route employed to fabricate the porous SiC preforms was provided in an earlier publication.<sup>8</sup> Two different polymer waxes were used as pore formers—bigger viscowax<sup>TM</sup> (abbreviated as VW in the following) (density 0.93–0.95 g/cc and diameter ~150  $\mu\text{m}$ , from Innospec Inc., Germany) and finer ceridust<sup>TM</sup> (abbreviated as CD in the following) (density 0.96–0.98 g/cc and diameter 7.5–9.5  $\mu\text{m}$ , from Clariant AG, Switzerland). To vary the overall SiC content, preforms were fabricated with various SiC powder/wax mixture ratios ranging from 30/70 (lowest SiC content) to 70/30 (highest SiC content). To vary the pore morphology, five different mixture ratios of the two wax types were used (VW/CD = 1/0, 2/1, 1/1, 1/2, and 0/1) for each SiC/wax mixture. After mixing the SiC powder (Amperpress UF-15-Premix, H. C. Starck, Germany with density 3.15 g/cc) with the pore formers using dry ball milling, the mixture was pressed into cylindrical preforms under 40 MPa uniaxial pressure. To further investigate the influence of the applied uniaxial pressure, additional preforms were made from one powder mixture type (SiC/wax = 50/50 with VW/CD = 1/1) under different uniaxial pressures between 10 and 80 MPa. The nominal length and diameter of the green

C.-H. Hsueh—contributing editor

\*Member, The American Ceramic Society.

\*\*Fellow, The American Ceramic Society.

<sup>†</sup>Author to whom correspondence should be addressed. e-mail: Siddhartha.roy@kit.edu

tablets were 9 mm and 24 mm, respectively. All samples were additionally cold isostatic pressed under 400 MPa. The green preforms were subsequently heated to 800°C to pyrolyse the polymer wax to generate the porosity and finally sintered at 2050°C for 30 min. Both heating and sintering were carried out in argon atmosphere. Four preforms were fabricated for each powder mixture type. Densities of the porous preforms were measured according to Archimedes principle by immersing in distilled water.

## (2) SEM Images

2D and 3D structural analyses of the preforms were carried out in Ref. [8] Representative SEM images of the preforms fabricated using various VW/CD mixture ratios and for 50/50 ratio of SiC/wax are shown in Fig. 1 to further discuss the main features of the respective microstructures. The preforms, whose micrographs are shown in this figure, were pressed uniaxially under 40 MPa and the vertical direction in each micrograph corresponds to the pressing direction.

These SEM images show that for the same total wax content, the type of wax mixture used has a significant influence on the preform architecture. Preforms fabricated using only the larger VW wax particles as pore formers [Fig. 1(a)] exhibit large spherical to elliptical pores with the pore size similar to the diameter of the original wax particles. In addition, several long cracks joining individual large pores, probably formed during volume expansion of wax particles during melting and decomposing are also observed. In preforms

made using only finer CD wax particles [Fig. 1(e)] a fine network pore structure is observed. A few large pores are also visible. These were generated due to agglomeration of CD wax particles during initial dry mixing of the powders. These pores are also flattened under the influence of the uniaxial pressure. Preforms fabricated using a mixture of the two wax types [Figs. 1(b)–(d)] show a trimodal pore distribution (spherical to elliptical pores from VW, fine network pores from CD, and large pores from CD agglomerates). In addition, the fine pore network in preforms with CD wax allows the molten wax and its gaseous decomposition products to flow out during fabrication and hence, no large cracks are observed in these preforms.

## (3) Determination of Elastic Properties Using Ultrasound Phase Spectroscopy

One sample of each preform type was studied to investigate the influence of the processing parameters on their elastic properties. Measurements were carried out on rectangular parallelepiped samples with nominal dimensions 7 mm × 5 mm × 5 mm with the long axis along the uniaxial press direction. The coordinate system introduced in Ref. [8] was also used in this work—the uniaxial press direction in each sample was taken as direction 1, whereas the two directions orthogonal to this direction were taken as directions 2 and 3, respectively.

The three longitudinal ( $C_{ii}$ ,  $i = 1-3$ ) and the three shear ( $C_{ii}$ ,  $i = 4-6$ ) elastic constants in each sample were

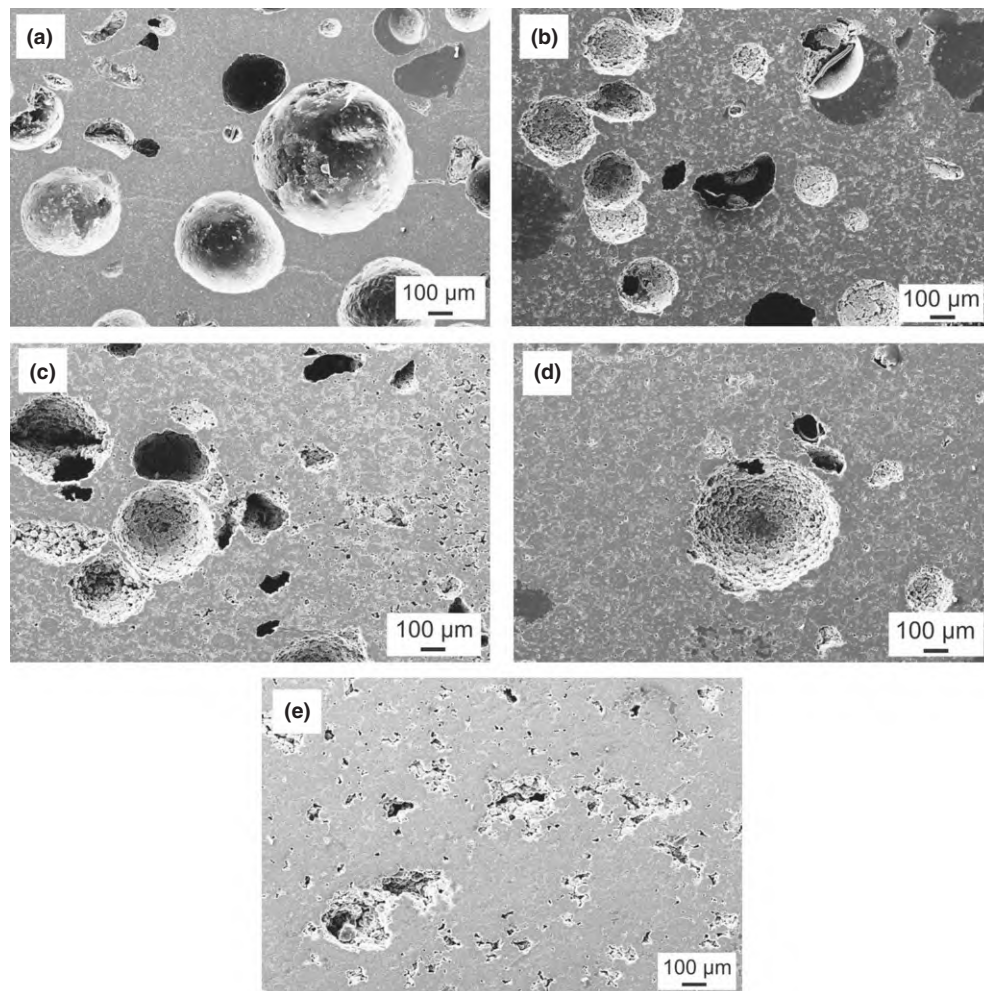


**Fig. 1.** Representative SEM images of the porous preforms fabricated using various mixture ratios of the two wax types for a SiC/wax powder ratio 50/50. (a) VW/CD = 1/0, (b) VW/CD = 2/1, (c) VW/CD = 1/1, (d) VW/CD = 1/2, and (e) VW/CD = 0/1. The micrographs show the face parallel to the direction of uni-axial pressing.

determined using ultrasound phase spectroscopy (UPS) following the methodology described in detail in Ref. [8]. Group velocities ( $V$ ) of waves were determined by measuring the slopes of the respective phase shift versus frequency spectra. Measurements were carried out within the frequency range of 10 kHz to 2–5 MHz. The elastic constants were determined from measured density and wave velocity by the following relation:

$$C_{ii} = \rho \cdot V^2 \quad (1)$$

where  $\rho$  is the sample density. For the three longitudinal elastic constants  $C_{11}$ ,  $C_{22}$ , and  $C_{33}$  the longitudinal wave velocities were determined along directions 1, 2, and 3, respectively. Each shear elastic constant was determined from the average of two different shear wave velocities. For  $C_{44}$ ,  $C_{55}$ , and  $C_{66}$  these velocities were  $V_{23}$  and  $V_{32}$ ,  $V_{13}$  and  $V_{31}$ , and  $V_{12}$  and  $V_{21}$  (the first suffix denoting the direction of wave propagation and the second suffix denoting the direction of vibration of the particles of the medium<sup>11</sup>), respectively.

### III. Results and Discussions

#### (1) Structural Analysis

For each preform, the total porosity (in vol%) was calculated from the measured density following the relation:

$$V_p = \left(1 - \frac{\rho}{\rho_s}\right) \times 100 \quad (2)$$

where  $V_p$  is the total porosity,  $\rho$  is the preform density which is determined following Archimedes principle, and  $\rho_s$  is the density of SiC. Average total porosities for all preform types were calculated. The data points in Fig. 2 show the average total porosity plotted against the wax ratio (VW/CD) for different SiC/wax ratios in the initial powder mixture. The error bars in the plot denote one standard deviation in total porosity within a particular preform type. For mixtures with high total wax content and a relatively high amount of CD wax (VW/CD = 0/1 for 40/60 SiC/wax mixture type and VW/CD = 1/2 and 0/1 for 30/70 SiC/wax mixture type), the preforms were not sufficiently consolidated from mechanical point of view to sustain handling and their densities could not be measured.

As discussed in Ref. [8], Fig. 2 shows that the total porosity depends only on the SiC/wax powder ratio in the initial mixture, with the amount and the type of wax used having no significant influence. The rate of increase in total porosity

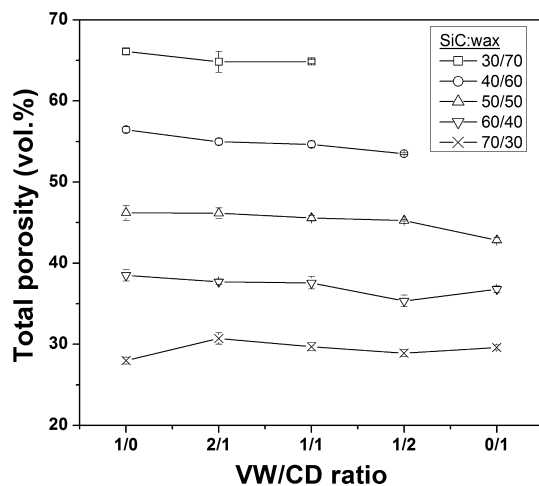


Fig. 2. Vol% porosity as a function of VW/CD ratio for different SiC/wax ratios in the initial powder mixture.

with increasing total wax content in the mixture is similar for the complete range of wax content studied.

#### (2) Effect of Porosity and Pore Morphology on Preform Elastic Properties

Figure 3 shows the effect of total porosity on the three longitudinal and the three shear elastic constants of the preforms. Each plot in the figure corresponds to a particular ratio between the two wax types in the initial powder mixture. No measurable phase spectrum could be obtained for the elastic constants  $C_{11}$ ,  $C_{44}$ ,  $C_{55}$ , and  $C_{66}$  for the preform fabricated with 30/70 SiC/wax powder mixture with VW/CD ratio 1/1; as well as for  $C_{44}$  for the preform fabricated with 70/30 SiC/wax powder mixture with VW/CD ratio 1/1. All five plots in the figure have been drawn to the same scale to facilitate comparison between various wax mixture types. The main observations from Fig. 3 are listed below:

1. Apart from  $C_{11}$  for a VW/CD ratio of 2/1, the elastic constants decrease with increasing total porosity.
2. Irrespective of porosity, the longitudinal elastic constants follow the general trend  $C_{11} < C_{22} \approx C_{33}$  and  $C_{44} > C_{55} \approx C_{66}$ . Hence, the preforms exhibit transverse isotropy with respect to the uniaxial press direction. Stiffness reduction along direction 1 results from flattening of the pores caused by uniaxial pressing and this has been discussed in detail in Ref. [8].
3. Among all mixture types, preforms with a VW/CD mixture ratio of 1/0 result into lowest values of  $C_{11}$  at all porosities. This drastic stiffness drop results from the long cracks present in this preform type [visible in Fig. 1(a)], mostly oriented perpendicularly to direction 1 (=preform press direction). Among preforms with VW/CD ratio 2/1,  $C_{11}$  in the preform with the lowest studied porosity (corresponding to 70/30 mixture of SiC/wax) lies significantly below the expected trend. This anomalous trend can also be explained by the presence of cracks in this preform. As shown in Fig. 1, in preforms with 50/50 ratio of SiC/wax, introduction of fine CD wax in the powder mixture generates a fine network pore structure and hence, the molten wax does not crack the preform as it flows out. This observation also holds for preforms with higher total wax content. However, at significantly lower total wax content, the smaller amount of fine CD wax in the green bodies provides insufficient network pores for the molten wax to flow out. Hence, cracks similar to preforms with only VW wax develop. One representative SEM image of the face parallel to the pressing direction for this preform is shown in Fig. 4. However, due to the fewer number of these cracks,  $C_{11}$  in this sample is almost twice than the corresponding sample with only VW wax with similar total porosity.
4. For all porosities, lowest values of the elastic constants  $C_{22}$ – $C_{66}$  are obtained for preforms prepared using only CD wax. This can be attributed to the fine network pore structure and the large pores resulting from CD agglomerates.

Material property maps provide an effective way to compare various properties over a wide range of materials. Idea of these maps goes back to Ashby.<sup>12</sup> Figure 5 shows typical examples of such plots where Young's modulus (left-hand side) and shear modulus (right-hand side) have been plotted against density. These plots were made using the material database package CES EduPack.<sup>13</sup> In making the plot for Young's modulus, no distinction has been made between  $C_{ii}$  ( $i = 1-3$ ) and Young's modulus. However, as discussed by Wanner,<sup>14</sup> the error associated with this simplification only has a minor influence. These plots are drawn in log–log scale and this allows plotting the complete sphere of the available materials—ranging from the flimsiest foams to the stiffest ceramics or the heaviest metals. Different colored bubbles in

the plot earmark the main material groups. The region covered by the porous SiC preforms studied in this work is marked in each plot using dark bordered ellipse. Following Eq. (1), for constant wave velocity, double log plot of elastic constant versus density results into straight lines with slope equal to unity. Contours of constant wave velocities are shown in each plot as dashed lines. The plots show that the velocities of the longitudinal and the shear waves propagating through the studied porous preforms lie between those of the most compliant metals and the stiffer technical ceramics.

Although both stiffness and density decrease with increasing porosity, their dependence on porosity is different. Density depends only on the amount of porosity, whereas stiffness depends both on its amount and type (pore shape, pore size, distribution, etc.). The effect of porosity on stiffness has been intensively studied and several model expressions have been proposed. A description of these models is outside the scope of this work and this can be found in monographs

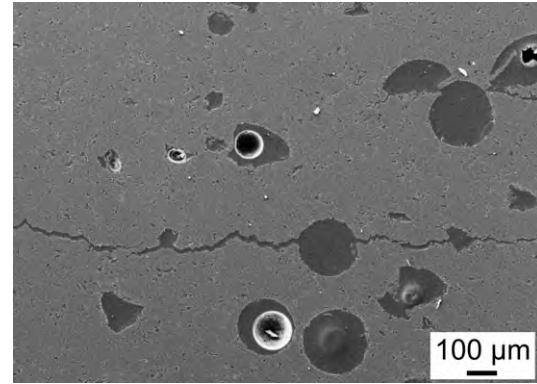


Fig. 4. Representative SEM image of the face parallel to the uniaxial press direction for the preform fabricated from a 70/30 mixture ratio of SiC/wax with 2/1 ratio of VW/CD wax.

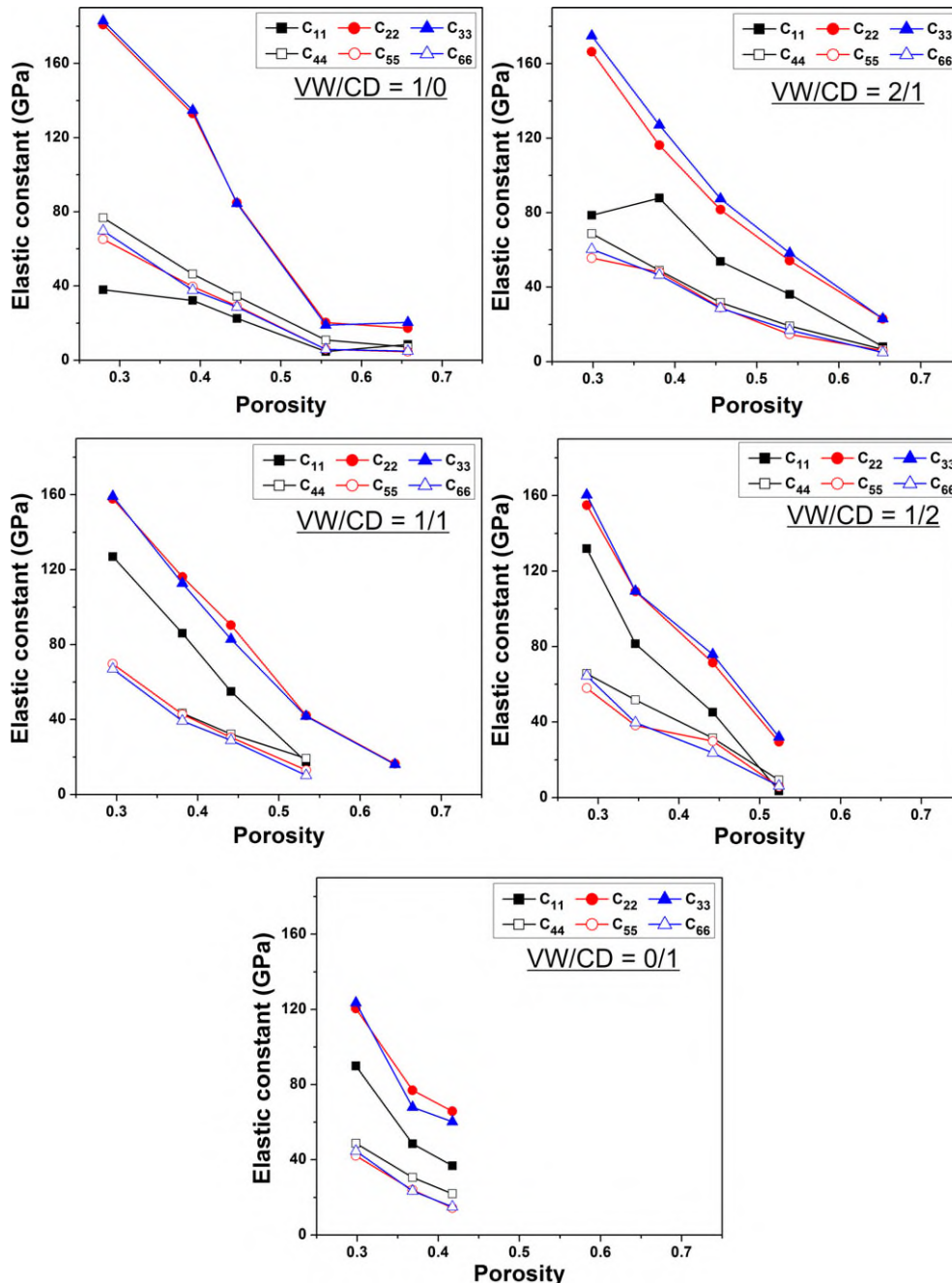
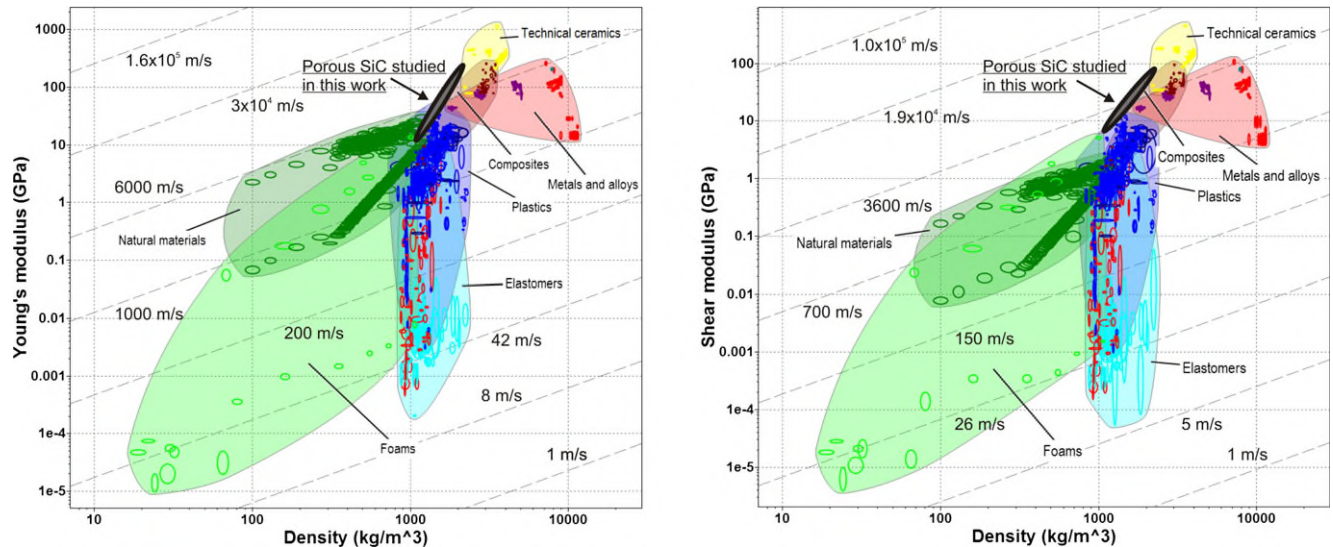


Fig. 3. Effect of porosity on the longitudinal and the shear elastic constants of the preforms. Plots for all five mixture ratios between the two wax types in the initial powder mixture are shown.



**Fig. 5.** Material property maps. Young's modulus is plotted against density in the left hand side plot while shear modulus is plotted against density in the right hand side plot. Big bubbles in each plot denote the main material classes. Contours denoting same velocity are also plotted as dashed lines. Regions in these plots, covered by the porous preforms studied in this work are marked in each plot as dark bordered ellipses.

written by Rice.<sup>15,16</sup> Among these, the models based on minimum solid area (MSA) predict up to a critical intermediate porosity level ( $P_c$ ) a simple  $\exp(-b \cdot P)$  dependence of the property over porosity ( $P$ ).<sup>15,17</sup> A semilog plot with the absolute or the relative property in log scale to the porosity in linear scale typically results into a straight line with slope  $-b$  up to a porosity  $P_c$ . The value of  $b$  typically lies between 2 and 7. A thorough theoretical analysis of the dependence of  $b$  on pore shape and size has been carried out by Andersson,<sup>18</sup> whereas Rice<sup>19</sup> reported a compilation of the experimentally determined  $b$  values for various porous ceramic types. Both  $b$  and  $P_c$  were calculated for the three longitudinal and the three shear elastic constants in all preforms studied in this work. To do this, elastic properties of bulk SiC (used as elastic properties at zero porosity) were calculated assuming isotropy and using 400 GPa, 0.14, and 175 GPa as its Young's modulus, Poisson's ratio, and shear modulus, respectively.<sup>13</sup> Figure 6 shows a representative plot for calculation of  $b$  and  $P_c$  for the elastic constant  $C_{22}$  in the preform fabricated using 2/1 mixture of VW/CD and Table I lists these values for different VW/CD mixture ratios in the initial powder mixtures.

The table shows that apart from  $C_{11}$ , for all other elastic constants and for all VW/CD ratios,  $b$  lies between 2.9 and 4.5. Highest  $b$  is obtained for  $C_{11}$  in the preform fabricated using only VW wax and this can be explained by the long cracks present in this preform. Andersson<sup>18</sup> has provided detail theoretical analysis of the influence of such cracks on stiffness of the body containing them and has shown that when measurement is carried out normal to such cracks,  $b$  approaches infinity as the aspect ratio of the cracks (length/thickness) approaches zero. Table I further shows that in all samples and for all elastic constants,  $P_c$  lies between 0.28 and 0.44. Although Table I is useful for a discussion of the effect of porosity distribution on stiffness of the porous SiC preforms; a drawback of the above analysis is the lack of any data at lower porosities between 0 and 0.28. To do this, preforms need to be fabricated with even higher SiC/wax ratio; which was outside the scope of this work.

### (3) Evolution of Preform Elastic Anisotropy

Figure 3 shows that the dependence of the elastic constants on porosity is different for various mixture ratios of the two wax types in the powder mixture. To understand how different mixture ratios affect the individual elastic constants, a study of the evolution of the anisotropy between the elastic constant along the uniaxial press direction and the constants

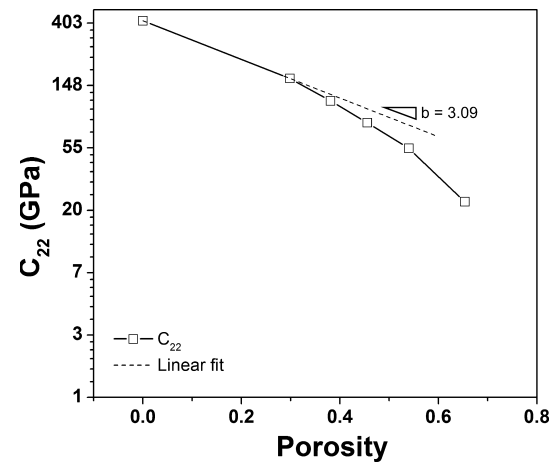


**Fig. 6.** Representative plot showing the calculation of  $b$  and  $P_c$  for  $C_{22}$  in the preform fabricated using a VW/CD ratio of 2/1.

along the two transverse directions is necessary. The anisotropy ratio (AR) is defined in this work as follows:

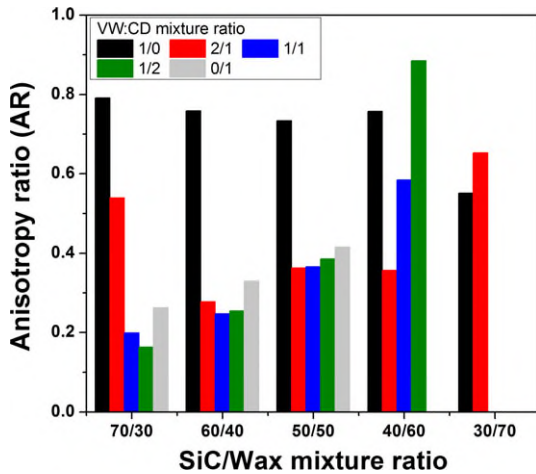
$$AR = \frac{\text{Average}(C_{22}, C_{33}) - C_{11}}{\text{Average}(C_{22}, C_{33})} \quad (3)$$

Figure 7 plots AR as a function of SiC/wax ratio for various mixtures of the two wax types in the powder mixture. The main observations from this figure are listed below:

1. If individual VW/CD mixture ratios are considered, then over the complete porosity range the highest anisotropy is obtained for the 1/0 mixture. This is due to the very low stiffness of these preforms along the press direction due to the presence of the long cracks normal to this direction.
2. Apart from the preform made using VW/CD ratio 2/1 and SiC/wax ratio 70/30; for all SiC/wax mixture types the lowest anisotropy is observed in preforms with 2/1 and 1/1 ratios of VW/CD.
3. For preforms with more than 50 vol% total wax content, a general increase in anisotropy is observed with an increase in CD wax content in the powder mixture. Figure 3 further shows that for the 30/70 SiC/wax mixture, this increase in anisotropy is associated with a decrease in all elastic constants. This can be attributed to the com-

**Table I. Calculated Values for  $b$  and  $P_c$  for the Three Longitudinal and the Three Shear Elastic Constants as a Function of VW/CD Mixture Ratio in the Initial Powder Mixture**

	VW:CD = 1:0		VW:CD = 2:1		VW:CD = 1:1		VW:CD = 1:2		VW:CD = 0:1	
	$b$	$P_c$	$b$	$P_c$	$b$	$P_c$	$b$	$P_c$	$b$	$P_c$
$C_{11}$	8.6	0.28	5.6	0.3	4.12	0.38	4.04	0.29	5.16	0.3
$C_{22}$	2.95	0.39	3.09	0.3	3.43	0.41	3.48	0.29	4.18	0.3
$C_{33}$	2.92	0.39	2.93	0.3	3.27	0.3	3.36	0.29	4.09	0.3
$C_{44}$	2.95	0.28	3.13	0.3	—	—	3.43	0.3	4.27	0.3
$C_{55}$	3.53	0.28	3.84	0.3	3.10	0.3	3.87	0.29	4.78	0.3
$C_{66}$	3.37	0.39	3.5	0.38	3.25	0.3	3.47	0.34	4.55	0.3



**Fig. 7.** Evolution of the preform anisotropy as a function of SiC/wax mixture ratio for various ratios of VW/CD in the initial powder mixture.

bin influence of the fine network pore structure and the presence of large mm sized pores.

- For preforms with a mixture of the two wax types, anisotropy generally increases with increasing total wax content in the initial mixture.

The above discussion typically shows that the pores resulting from various mixture ratios of the two wax types affect the elastic properties differently over the broad range of porosities studied in this work. Preforms fabricated using only VW wax show high anisotropy, whereas only CD wax at high wax contents gives fragile preforms. To obtain optimum elastic properties along all directions, preforms need to be fabricated using a mixture of the two wax types. In preforms with low total porosity (high SiC/wax ratio) the VW/CD ratio should be low, whereas in preforms with high total porosity (low SiC/wax ratio) the VW/CD ratio should be high. In Fig. 8, these inferences have been summarized in the form of a map, where elastic properties and initial powder mixture are combined. This map facilitates easy visual selection of the initial powder mixture to fabricate porous preforms with tailor-made elastic properties.

#### (4) Effect of Applied Uniaxial Pressure

Lastly, as the anisotropy in these preforms results from the initial applied uniaxial pressure; it is interesting to investigate the effect of this pressure on the preform elastic properties. To do this, preforms were fabricated using 50/50 SiC/wax mixture with 1/1 ratio of VW/CD under various uniaxial pressures between 10 and 80 MPa. The three longitudinal elastic constants of each preform were measured. Figure 9 plots the densities, the three longitudinal elastic constants as well as the AR [calculated according to Eq. (3)] of these preforms as a function of the uniaxial pressure. The plot shows that the preform density is independent of the uniaxial pres-

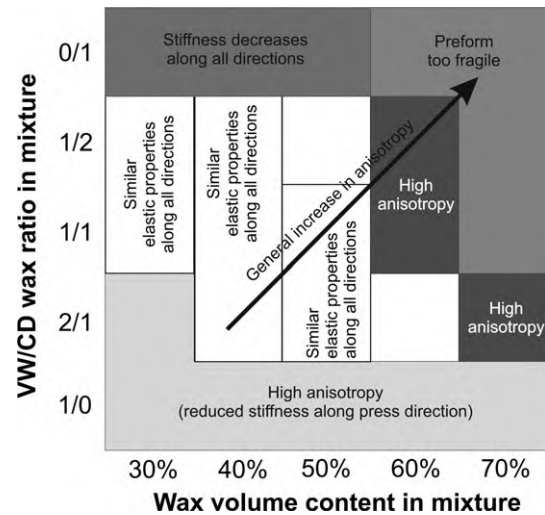


**Fig. 8.** Elastic property versus powder mixture map for the porous preforms.

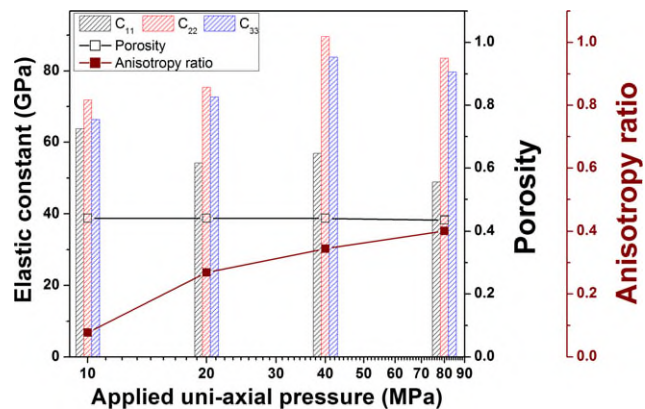


**Fig. 9.** Effect of the applied initial uni-axial pressure on the porosity, the three longitudinal elastic constants and the anisotropy of the preforms fabricated using 50/50 ratio of SiC/wax with 1/1 ratio of VW/CD.

sure. The longitudinal elastic constant along press direction continuously decreases and the longitudinal elastic constants along directions 2 and 3 increase with increasing uniaxial pressure. Hence, the preform anisotropy increases monotonically with increasing uniaxial pressure; though the symmetry of the preforms remains unchanged.

## V. Conclusions

Thorough analyses of the elastic properties of open porous silicon carbide preforms have been carried out in this work using ultrasound phase spectroscopy. The main conclusions from this study are summarized below:

Both the longitudinal and the shear elastic constants decreased with increasing porosity in the preforms. Up to an intermediate porosity ( $P_c$ ), the rate of decrease in the elastic constants with porosity followed a simple  $\exp(-b*P)$  dependence with  $b$  lying mostly in the range of 2.9–4.5.

Uniaxial pressure applied to the powder mixture prior to cold isostatic pressing and sintering flattens the pores along the press direction and this reduces the stiffness of the preforms along this direction. The degree of anisotropy depends both on the amount of porosity and the pore structure. For the complete range of porosity studied, preforms fabricated using a mixture of the two wax types show less anisotropy than the preforms fabricated using only one type of pore former. A high volume fraction of smaller pore formers at lower porosities and a high volume fraction of larger pore formers at higher porosities lead to preforms with optimum elastic properties along all directions.

Based upon these results, an elastic anisotropy—powder mixture map has been proposed to describe the dependence of the preform elastic properties on the type of powder mixture used.

While the porosity of the preforms is independent of the initial uniaxial pressure, the preform anisotropy is directly proportional to it.

This study shows that it is possible to fabricate silicon carbide preforms with various degrees of elastic anisotropy by simply varying the composition of the initial powder mixture used. In our future work these preforms will be infiltrated with aluminum alloy to fabricate metal/ceramic composites to further investigate the influence of the phase morphology on the composite thermomechanical properties.

### Acknowledgments

The authors thank TER HELL & CO. GmbH for providing them with the polymer waxes free of cost and Mr. Pascal Hettich for his assistance in processing and characterization of the porous preforms. The work was carried out within the scope of German Research Foundation (DFG), grant no. RO 4164/1-1.

### References

- <sup>1</sup>M. Kouzeli and D. C. Dunand, "Effect of Reinforcement Connectivity on the Elasto-Plastic Behavior of Aluminum Composites Containing Sub-Micron Alumina Particles," *Acta Mater.*, **51**, 6105–21 (2003).
- <sup>2</sup>G. Roudini, R. Tavangar, L. Weber, and A. Mortensen, "Influence of Reinforcement Contiguity on the Thermal Expansion of Alumina Particle Reinforced Aluminum Composites," *Int. J. Mater. Res.*, **101**, 1113–20 (2010).
- <sup>3</sup>T. Huber, H. P. Degischer, G. Lefranc, and T. Schmitt, "Thermal Expansion Studies on Aluminium-Matrix Composites With Different Reinforcement Architecture of SiC Particles," *Compos. Sci. Technol.*, **66**, 2206–17 (2006).
- <sup>4</sup>S. Roy, J. Gibmeier, V. Kostov, K. A. Weidenmann, A. Nagel, and A. Wanner, "Internal Load Transfer in a Metal Matrix Composite With a Three-Dimensional Interpenetrating Structure," *Acta Mater.*, **59**, 1424–35 (2011).
- <sup>5</sup>A. Mattern, B. Huchler, D. Staudenecker, R. Oberacker, A. Nagel, and M. J. Hoffmann, "Preparation of Interpenetrating Ceramic-Metal Composites," *J. Eur. Ceram. Soc.*, **24**, 3399–408 (2004).
- <sup>6</sup>C. Zweben, "Advances in Composite Materials for Thermal Management in Electronic Packaging," *JOM*, **50**, 47–51 (1998).
- <sup>7</sup>C. Zweben, "Metal-Matrix Composites for Electronic Packaging," *JOM*, **44**, 15–23 (1992).
- <sup>8</sup>S. Roy, K. G. Schell, E. C. Bucharsky, P. Hettich, S. Dietrich, K. A. Weidenmann, A. Wanner, and M. J. Hoffmann, "Processing and Elastic Property Characterisation of Porous SiC Preform for Interpenetrating Metal/Ceramic Composites," *J. Am. Ceram. Soc.*, **95**[10], 3078–83 (2012).
- <sup>9</sup>S. Roy, O. Stoll, K. A. Weidenmann, A. Nagel, and A. Wanner, "Analysis of the Elastic Properties of an Interpenetrating AlSi12–Al<sub>2</sub>O<sub>3</sub> Composite Using Ultrasound Phase Spectroscopy," *Compos. Sci. Technol.*, **71**, 962–8 (2011).
- <sup>10</sup>S. Roy and A. Wanner, "Metal/Ceramic Composites From Freeze-Cast Ceramic Preforms/Domain Structure and Elastic Properties," *Compos. Sci. Technol.*, **68**, 1136–43 (2008).
- <sup>11</sup>J. L. Rose, *Ultrasonic Waves in Solid Media*. Cambridge University Press, Cambridge, UK, 1999.
- <sup>12</sup>M. F. Ashby, "On the Engineering Properties of Materials," *Acta Metall.*, **37**, 1273–93 (1989).
- <sup>13</sup>CES Edupack, Granta Design Ltd., Cambridge, UK, 2008.
- <sup>14</sup>A. Wanner, "Elastic Modulus Measurements of Extremely Porous Ceramic Materials by Ultrasonic Phase Spectroscopy," *Mater. Sci. Eng., A*, **248**, 35–43 (1998).
- <sup>15</sup>R. W. Rice, *Porosity of Ceramics*. Marcel Dekker Inc., New York, 1998.
- <sup>16</sup>R. W. Rice, "The Porosity Dependence of Physical Properties of Materials/a Summary Review," *Key Eng. Mater.*, **115**, 1–20 (1996).
- <sup>17</sup>K. U. O'Kelly, A. J. Carr, and B. A. O. McCormack, "Minimum Solid Area Models Applied to the Prediction of Young's Modulus for Cancellous Bone," *J. Mater. Sci. - Mater. Med.*, **14**, 379–84 (2003).
- <sup>18</sup>C. A. Andersson, "Derivation of the Exponential Relation for the Effect of Ellipsoidal Porosity on Elastic Modulus," *J. Am. Ceram. Soc.*, **79**, 2181–4 (1996).
- <sup>19</sup>R. W. Rice, "Comparison of Physical Property-Porosity Behavior With Minimum Solid Area Models," *J. Mater. Sci.*, **31**, 1509–28 (1996). □